ELSEVIER

Thermochimica Acta 259 (1995) 1–12

thermochimica acta

Heat capacity measurement on ZrO_x ($x = 0$–0.31) from 325 to 905 K. Part I. Heat capacity anomaly due to thermal non-equilibrium state at low temperature ☆

Toshihide Tsuji*, Masaki Amaya

Department of Nuclear Engineering, Faculty of Engineering, Nagoya University, Furo-cho, Chikusa-ku, Nagoya 464-01, Japan

Received 22 July 1994; accepted 16 December 1994

Abstract

Heat capacities of ZrO_x($x = 0$–0.31) were measured from 325 to 905 K using an adiabatic scanning calorimeter. Two kinds of heat capacity anomalies were observed for all samples except pure zirconium metal. A λ-type heat capacity anomaly was observed in the temperature range from 600 to 750 K and was assigned to an order–disorder rearrangement of the interstitial oxygen atoms in zirconium host lattices. Another anomaly around 400–500 K depended on heating conditions, indicating that this anomaly is due to a non-equilibrium phenomenon. Due to the imperfect ordering of the sample during the cooling process, a temporary ordering and a subsequent recovery into an equilibrium state occur during the heating process at a finite rate, making a broad heat capacity anomaly. This behavior is discussed with reference to the results of the dependences of the cooling rate of the sample and the heating rate of the calorimeter on the heat capacity anomaly.

Keywords: Heat capacity; Heat capacity anomaly; Non-equilibrium state; order–disorder transition; Zirconium–oxygen alloy; ZrO_x

1. Introduction

The α-zirconium phase dissolves oxygen atoms up to 30 at% in the octahedral interstices of the hcp zirconium lattice at room temperature, forming ordered structures at higher oxygen compositions and lower temperatures. Yamaguchi [1], Hashimoto

☆ Presented at the 13th International Symposium on Chemical Thermodynamics, Clermont-Ferrand, France, 17–22 July 1994.

* Corresponding author.

SSDI 0040-6031(95)02264-3

[2] and Hirabayashi and coworkers [3–5] determined the ordered structures of zirconium–oxygen alloys by X-ray, electron and neutron diffraction methods. There are three phases with different degrees of order in the zirconium–oxygen system: the completely ordered phase α'', the intra-layer disordered phase α', and the completely disordered phase α. The α'' phase is further divided into $ZrO_{1/6}$, ZrO_x, LPSS and ZrO_z, where LPSS is the long-period stacking structure, and α' is represented as ZrO_y. The phase diagram in the Zr–O system determined by calorimetry, electrical resistivity measurement and neutron diffraction is shown in Fig. 1 [6]. Each region in Fig. 1 is distinguished by different types of oxygen occupancy of the three kinds of octahedral interstitial sites in a plane perpendicular to the c-axis and the stacking sequences of the planes parallel to the c-axis.

Heat capacity measurements can provide useful information for the transition mechanism by detecting the transition temperature and evaluating the transition enthalpy and entropy changes as a function of n_O/n_{Zr} ratio. Arai and Hirabayashi [6] measured the heat capacities of ZrO_x ($x = 0.16$–0.41) alloys and obtained enthalpy and entropy changes for the order–disorder transition. However, their results seem to have some ambiguities, since the heat capacity was not reported below 470 K, and the base line to estimate the entropy change due to the order–disorder transition was not clearly described. We also measured heat capacities of ZrO_x ($x = 0.17, 0.20, 0.28$ and 0.31) and $(Zr_{1-y}M_y)O_x$(M is Nb and Sn, $x = 0.17$ and 0.28, $y = 0$–0.07) from 325 to 905 K, using an adiabatic scanning calorimeter [7, 8]. Two kinds of heat capacity anomalies were observed for all samples: one was the anomaly at lower temperatures due to a non-

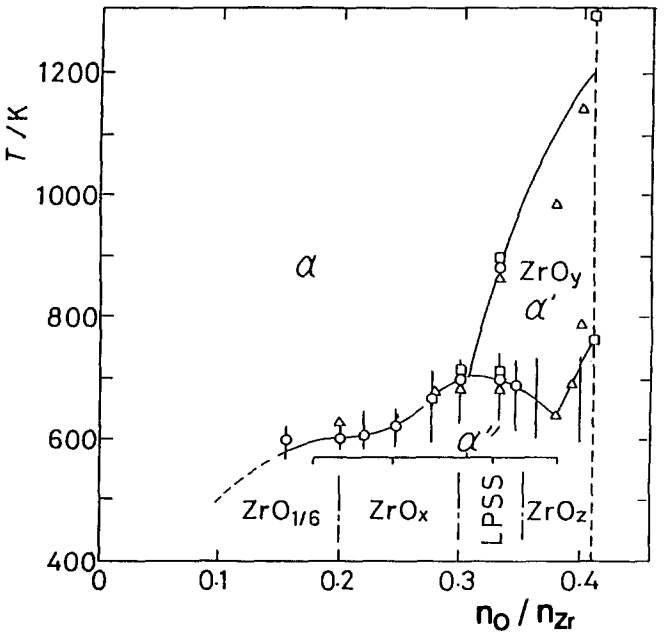

Fig. 1. Phase diagram in the Zr–O system [6]: ○, calorimetry; △, electrical resistivity measurement; □, neutron diffraction.

equilibrium phenomenon which was not reported by Arai and Hirabayashi [6]; and the other was the λ-type anomaly at higher temperatures assigned to an order–disorder rearrangement of oxygen atoms. The measured entropy change due to the order–disorder transition for Zr–O solid solution in our previous work was larger than that of Arai and Hirabayashi [6], but was in fairly good agreement with the theoretical value.

In this paper, heat capacities of ZrO_x ($x = 0$–0.31), having various n_O/n_{Zr} ratios, were measured from 325 to 905 K by an adiabatic scanning calorimeter. Before the λ-type heat capacity anomaly at high temperature, the heat capacity anomaly at low temperature due to a non-equilibrium phenomenon was observed. The measured heat capacities were abnormally small around the starting temperatures, increased rapidly, and then showed a broad peak. Here we will discuss this non-equilibrium phenomenon observed in the heat capacity measurement. The λ-type anomaly at high temperature assigned to an order–disorder rearrangement of oxygen atoms will be discussed in Part II of this study [9].

2. Experimental

2.1. Sample preparation

ZrO_x ($x = 0$–0.31) samples were prepared by using a method similar to the one used to prepare zirconium–oxygen alloys in an earlier study [7]. Zirconium metal sponge of 99.6% purity, containing the impurities Hf, Fe, O, N, etc., and zirconium metal oxidized at 773 K in air were mixed in an appropriate ratio and melted a few times using a plasma jet furnace under an Ar gas stream. The cast sample obtained was annealed for 3 days at 1273 K in an evacuated and sealed quartz tube, and cooled to room temperature over a period of 3 days. The sample was crushed into pieces of less than 3 mm size using a stainless-steel mortar. The crushed sample of about 20 g was sealed in a quartz vessel filled with He gas at 20 kPa, and annealed at 873 K for 2 weeks, then 500 K for 2 weeks and cooled slowly to room temperature over a period of 3 days to obtain a highly ordered phase; this sample was used for the heat capacity measurements. The identification of the phase and the measurement of lattice constants of the samples were carried out by X-ray diffractometry. The n_O/n_{Zr} ratio of the sample was determined from the weight gain by oxidizing it to ZrO_2 at 1273 K in air for 1 week.

2.2. Heat capacity measurement

The heat capacities of ZrO_x ($x = 0$–0.31) samples were measured using an adiabatic scanning calorimeter [10]; in this calorimeter the power supplied to the sample was measured continuously, and the heating rate was kept constant regardless of the kind and amount of the sample. The heating rate chosen was 1–4 K min^{-1}, and the measurement was carried out between 325 and 905 K under a pressure of about 130 Pa of air, using a sample of about 20 g sealed in a quartz vessel filled with He gas at 20 kPa. The heating rate and adiabatic control were usually maintained within ± 0.005 K min^{-1} and ± 0.01 K, respectively. The heat capacity measurement was conducted within an imprecision of $\pm 2\%$ and an inaccuracy of $\pm 2\%$.

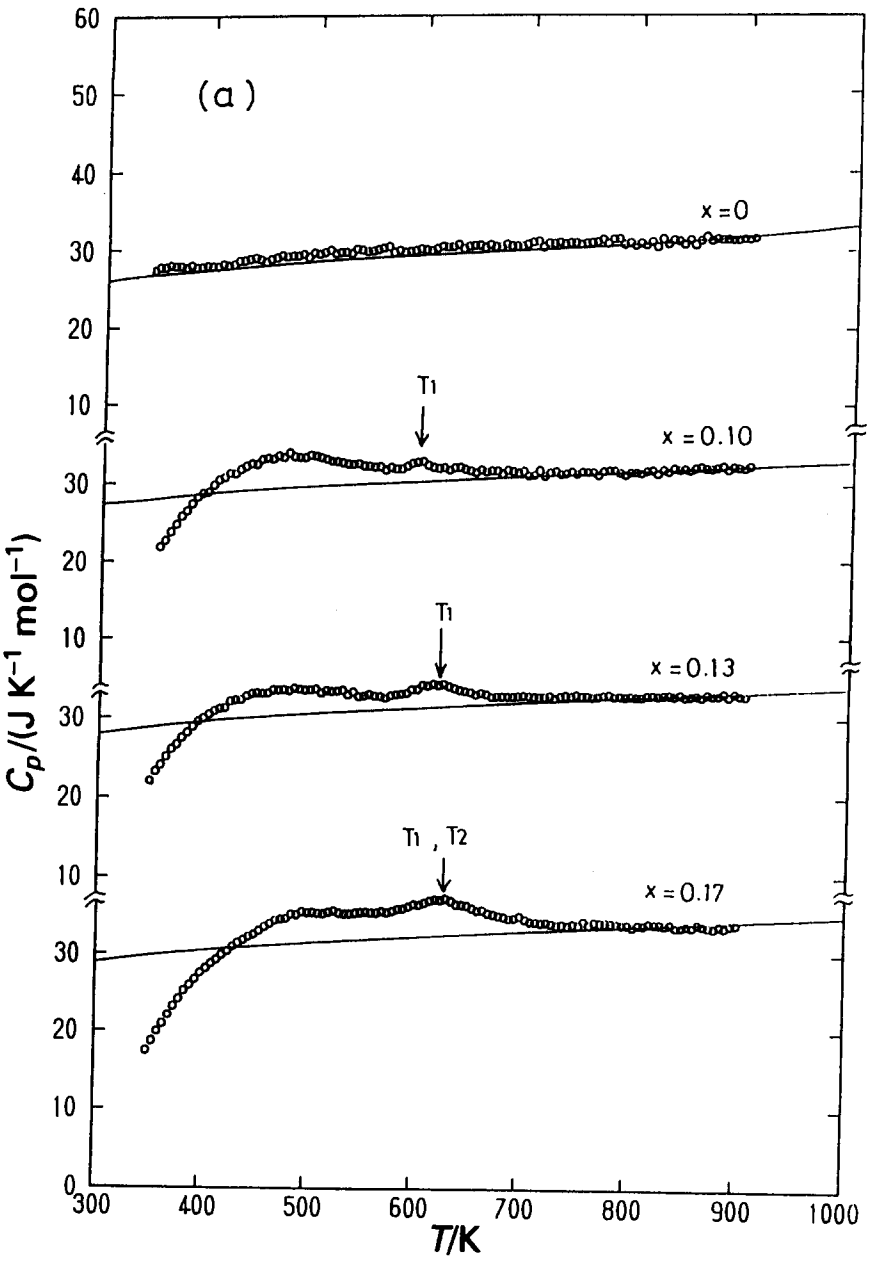

Fig. 2. (a) and (b). Heat capacities of ZrO_x ($x = 0, 0.10, 0.13, 0.17, 0.20, 0.24, 0.28$ and 0.31). The transition temperatures T_t are for the phase transition from the completely ordered phase α'' to the completely disordered phase α.

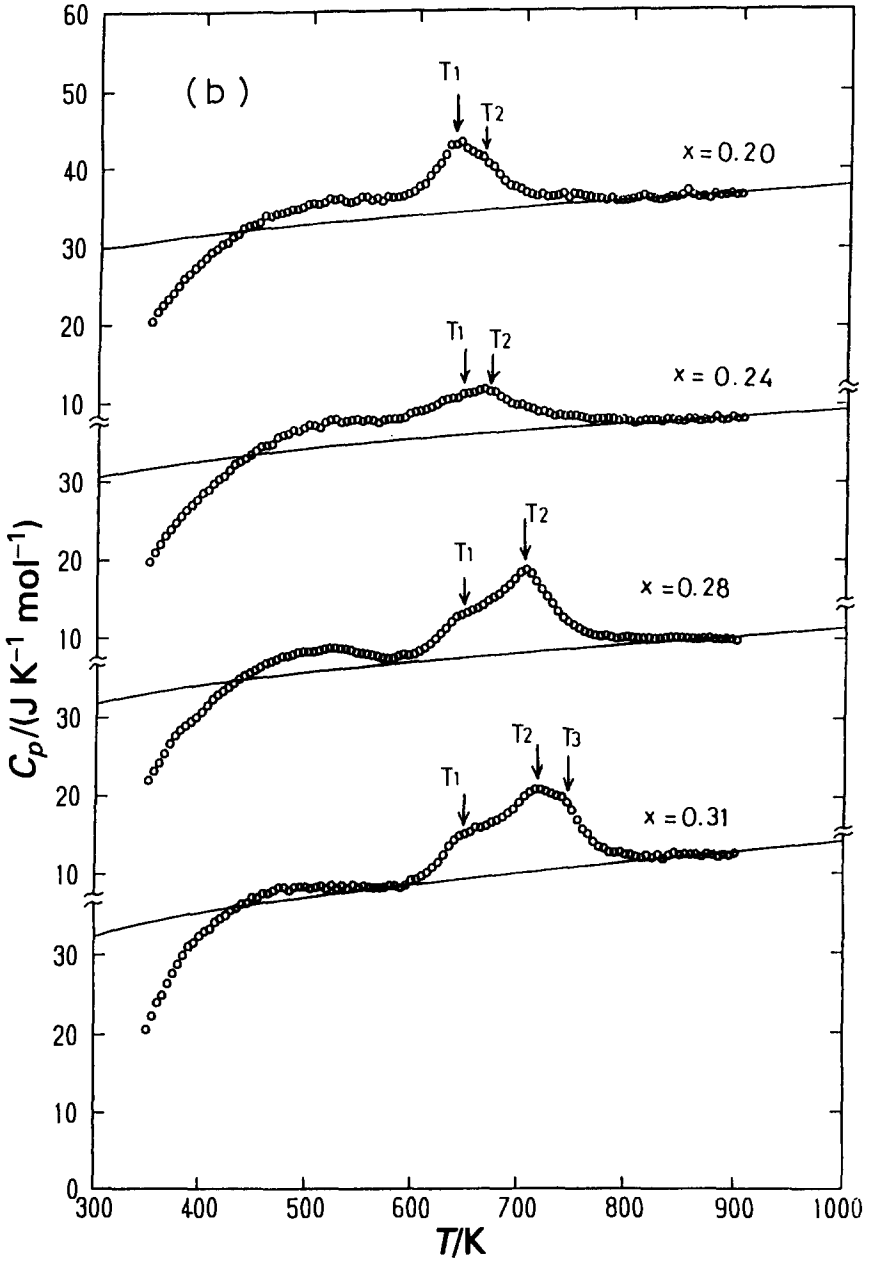

Fig. 2 *(continued)*

3. Results and discussion

Figs. 2(a) and (b) show the results of heat capacity measurements on ZrO_x (x = 0–0.31). As seen in the figure, the heat capacity data of pure zirconium metal measured

in this study are in good agreement with those reported by Douglas [11] (solid line for $x = 0$ in Fig. 2). The solid lines for all ZrO_x samples, except pure zirconium ($x = 0$), in Fig. 2 are the base lines of heat capacities which were estimated in a manner similar to that adopted in our previous study [7] and will be discussed in more detail in Part II of this study [9]. In Fig. 2, two kinds of heat capacity anomaly are seen for all the samples, except pure zirconium metal: a broad peak at about 500 K (low-temperature heat capacity anomaly) and the λ-type peak in the temperature range from 600 to 800 K (high-temperature heat capacity anomaly). The λ-type heat capacity anomalies at high temperature are assigned to an order–disorder rearrangement of interstitial oxygen atoms in the zirconium host lattice and will be discussed in Part II [9]. In this paper, the heat capacity anomaly at low temperature will be discussed.

The heat capacity curves at low temperature for ZrO_x ($x \neq 0$) samples show a strange behavior, as seen in Fig. 2. The much smaller heat capacity value compared with the base line and the presence of the broad peak indicate that heat release and heat absorption occur in addition to normal contributions to the heat capacity. As seen in Fig. 2, only pure zirconium metal fails to show any heat capacity anomaly, but all other samples ZrO_x ($x \neq 0$) show only one λ-type heat capacity anomaly and one or two additional humps in the curve, depending on the n_O/n_{Zr} ratio, at higher temperatures after a broad peak at low temperature. Thus the low temperature heat capacity anomaly at about 400–500 K seen in Fig. 2 is considered to be related to the movement of interstitial oxygen atoms in the zirconium host lattice. This type of abnormal heat capacity behavior at low temperature has also been observed in our laboratory for interstitial type V–O [12, 13], Ti–O [14], Zr–O [7], Zr–Nb–O [7] and Zr–Sn–O [8] solid solutions. In these solid solutions, the heat capacity anomaly at low temperature was always accompanied by the order–disorder transition at high temperature due to interstitial oxygen atoms or vacancy clusters. A similar abnormal behavior in the heat capacity has also been observed in substitutional ordered alloys, such as FeCo with a bcc structure [15], Cu_3Au [16] with fcc structure, and Mg_3Cd [17] with hcp structure, using a dynamic type of calorimeter. Such a behavior has been qualitatively explained by Sato and coworkers [18–20]. In their model, the degree of order in the alloy, which is determined only by the temperature in an equilibrium state, is regarded to change at a finite rate, controlled by a diffusion process, and the kinetics of the system can be described with the "path probability method" using the pair approximation. Although the model proposed by Sato and coworkers [18–20] has been applied to the substitutional alloy, a similar interpretation might be made for the interstitial-type zirconium–oxygen alloy, as follows. The temperature dependence of the configurational entropy of oxygen atoms in the zirconium host lattice is illustrated schematically in Fig. 3, where the solid curves indicate the temperature dependence of the entropy during cooling and heating at a finite rate, and the broken curve indicates the hypothetical equilibrium value. In the cooling process, the jump frequency of oxygen atoms decreases with decreasing temperature and the ordering of oxygen ceases below a critical temperature Tc_1, where the ordering rate controlled by the oxygen jump is very slow compared with the cooling rate. The ordering of oxygen is frozen in a non-equilibrium state ("frozen-in") where the entropy of the system is larger than the equilibrium value at the corresponding temperature; this state is preserved to room

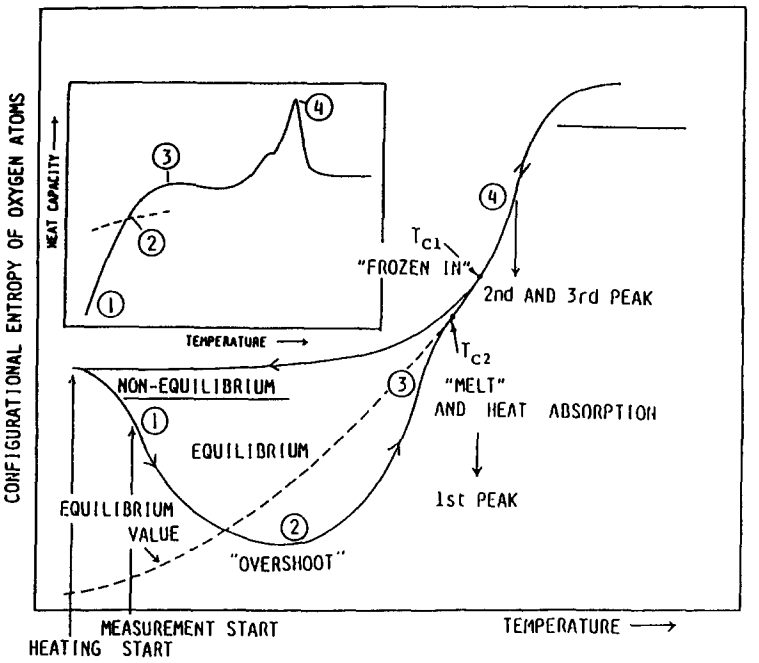

Fig. 3. Temperature dependence of configurational entropy of oxygen atoms.

temperature. Thus the sample itself is not really in an equilibrium state at the starting temperature at which the measurement is initially carried out. The ordering of oxygen atoms in the sample at the starting temperature is less than that at the hypothetical equilibrium state.

During the heating process, however, the degree of order increases from the "frozen-in" state to the equilibrium state with increasing temperature. Therefore, a lower heat capacity than the base line can be observed due to the heat release because of the ordering process. This type of oxygen atom movement does not occur gradually, but begins suddenly at a certain temperature where oxygen movement is possible after some relaxation time, which is necessary to achieve oxygen movement. As the temperature of the sample increases at a constant heating rate, the ordering of the oxygen atoms over-shoots the equilibrium value at a certain temperature, and then a higher order state than the equilibrium state can be achieved. At the temperature Tc_2, the ordering of oxygen atoms reaches the equilibrium state. These processes would result in the borad peak at low temperature. After that, the order–disorder transition is observed almost independently of this non-equilibrium phenomenon, except for the decrease in the entropy change due to the imperfect ordering at low temperatures.

In Fig. 2, the transition temperatures T_1, T_2 and T_3 for ZrO_x ($x = 0.10$–0.31) samples are phase transitions from the completely ordered phase α'' to the completely disordered phase α. A new phase diagram for the Zr–O system determined from these transition temperatures will be presented in Part II [9].

In order to confirm the model proposed by Sato and coworkers [18–20], heat capacity measurements for $ZrO_{0.28}$ samples with various ordered states at the starting temperature were made. Fig. 4 shows heat capacities for annealed, quickly cooled and quenched $ZrO_{0.28}$ samples at a heating rate of 2 K min^{-1}. The annealed sample was made by cooling slowly from 873 K, as described in detail in the experimental section. After the heat capacity measurement of the annealed sample from 325 to 905 K, the sample was quickly cooled to room temperature in the calorimeter by cutting off the power; this is the "quickly cooled" sample in Fig. 4. The quenched sample was formed by quenching from 873 K to liquid nitrogen temperature; this is the "quenched" sample in Fig. 4. As seen in Fig. 4, heat capacity curves with different thermal histories have the following characteristics. (a) Values of the heat capacity are abnormally small around the starting temperature and increase rapidly, followed by a broad peak at around 400–500 K. (b) After the broad peak, first and second peaks appear for the annealed sample, but only the second peak appears for the quickly cooled and quenched samples, becoming smaller with increasing cooling rate. (c) The heat capacity data agree well, irrespective of thermal history, after the order–disorder transition. In Fig. 4, the solid line is a heat capacity base-line.

Figs. 5(a) and (b) show the configurational enthalpy and entropy changes of the oxygens for $ZrO_{0.28}$ samples, calculated from the measured heat capacity data (C_{p_1}) and the base line (C_{p_2}) shown in Fig. 4 using the equations

$$H(T) - H(900) = \int_{900}^{T} (C_{p_1} - C_{p_2})\,\mathrm{d}T \tag{1}$$

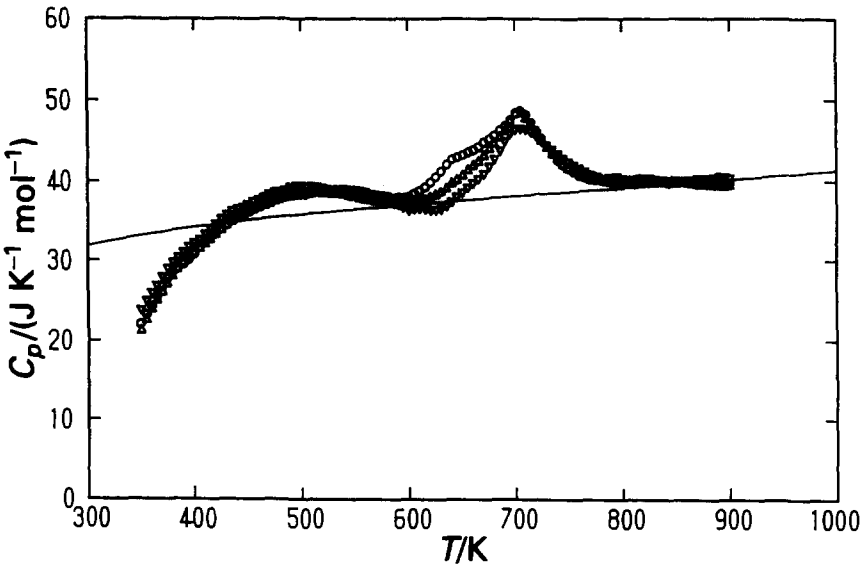

Fig. 4. Heat capacities of the annealed (○), quickly cooled (△) and quenched (▽) $ZrO_{0.28}$ samples.

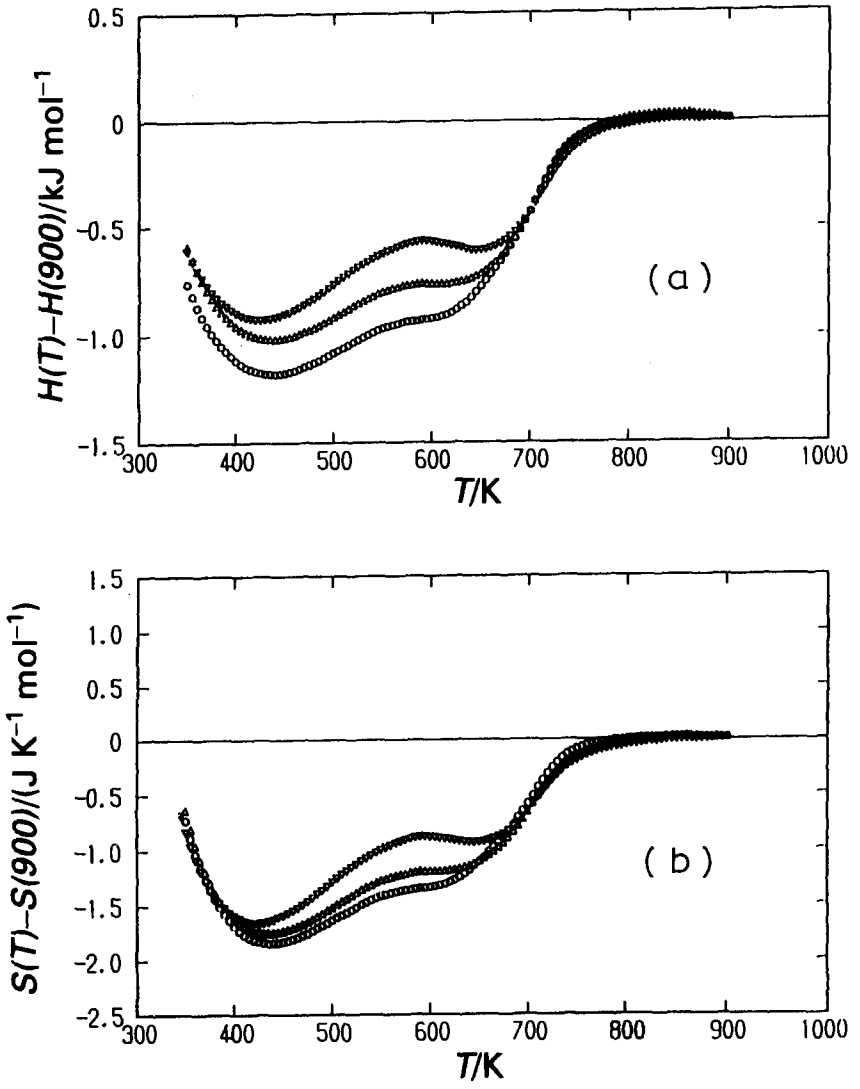

Fig. 5. (a) and (b). Plots of the configurational enthalpy and entropy changes of $ZrO_{0.28}$, respectively: ○, annealed; △, quickly cooled; and ▽, quenched $ZrO_{0.28}$ samples.

and

$$S(T) - S(900) = \int_{900}^{T} \{(C_{p_1} - C_{p_2})/T\}\, dT \tag{2}$$

where $H(T)$ and $H(900)$ are enthalpies at T and 900 K, respectively, and $S(T)$ and $S(900)$ are entropies at T and 900 K. Since the heat capacity data agree well irrespective of thermal history after the high-temperature phase transition, the disordered phases

are considered to be obtained after the order–disorder transition. Thus the values of $H(900)$ and $S(900)$ are assumed to be zero for the calculation of Eqs. (1) and (2). It is found from Figs. 5(a) and (b) that the configurational enthalpy and entropy changes of oxygen become smaller in the order: annealed, quickly cooled and quenched samples, depending on the cooling rate of sample preparation. This means that the ordering of oxygen atoms in the sample at room temperature decreases with increasing cooling rate due to the freezing of oxygen atom movement at higher temperatures. In the heating process, the configurational enthalpy and entropy of oxygen atoms for the annealed sample decrease with increasing temperature in the ordering direction as shown in Fig. 3. After overshooting the equilibrium state, the ordering process of oxygen atoms increases with increasing temperature, and then the configurational enthalpy and entropy changes decrease with further increasing temperature. However, the arrangements of the initial oxygen atoms for the quickly cooled and quenched samples are in a higher disorder state than that for the annealed sample due to the freezing of the oxygen atom movement at higher temperatures. These higher configurational enthalpy and entrpy changes at room temperature decrease with increasing temperature and the minima increase, as shown in Figs. 5(a) and (b).

Finally, in order to check the model proposed by Sato and coworkers [18–20], the heat capacity results for $ZrO_{0.28}$ samples are shown in Fig. 6 as a function of heating rate. The peak position of the heat capacity anomaly at low temperature shifts to higher temperature with increasing heating rate. Thus the heat capacity anomaly at low temperature overlaps the high-temperature heat capacity anomaly and both peak positions become unclear, especially at the heating rate of 4 K min^{-1}. Fig. 7 shows the

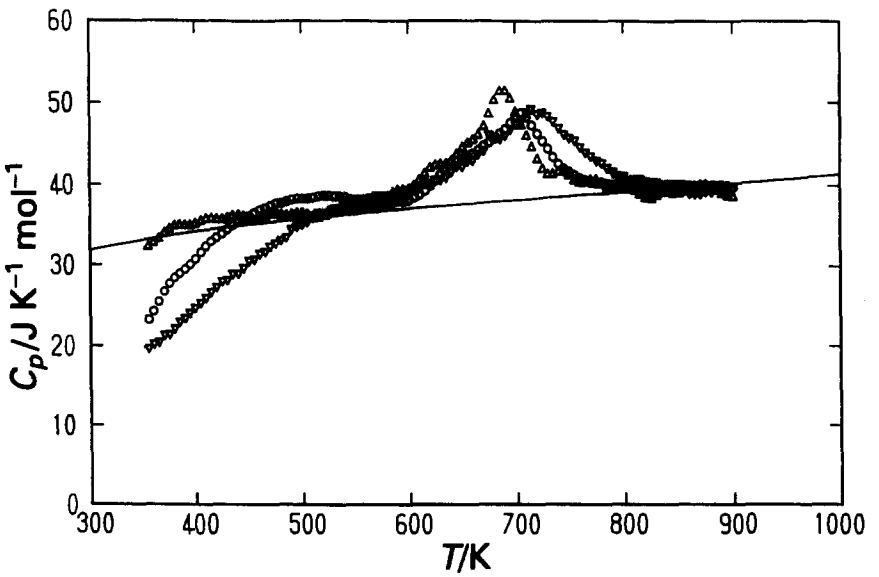

Fig. 6. Heat capacities of $ZrO_{0.28}$ samples as a function of heating rate: △, 1 K min^{-1}; ○, 2 K min^{-1}; ▽, 4 K min^{-1}.

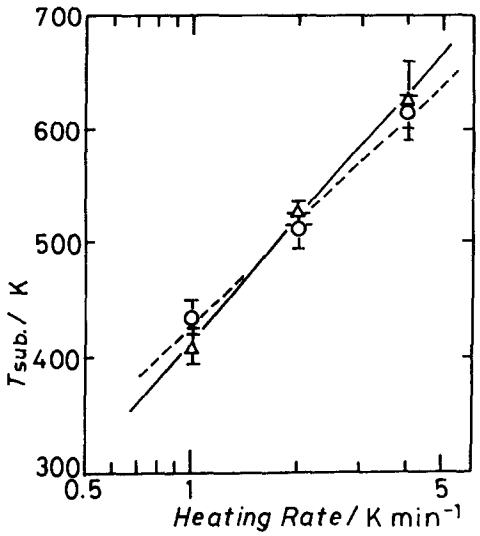

Fig. 7. Peak temperature plotted against heating rate for ZrO_x: ○, $ZrO_{0.17}$; △, $ZrO_{0.28}$.

peak temperature of the low-temperature heat capacity anomaly as a function of heating rate. A good linear relationship between the peak temperature and the logarithm of the heating rate is seen in the figure. The slope for an interstitial-type alloy obtained in this study is larger than that for the substitutional alloy Mg_3Cd [17]. This may be related to the difference in activation energy of the diffusing atoms. As seen in Fig. 7, the peak of the low-temperature heat capacity anomaly at the heating rate of 4 K min^{-1} is higher by about 100 K than that at 2 K min^{-1}. This suggests that the heat capacity anomaly at low temperature is caused by a non-equilibrium phenomenon and not by underlying sluggish phase transitions. This phenomenon is interpreted as follows. At the higher heating rate, the system is not in an equilibrium state until the sample reaches higher temperatures, because the rate process of the system is controlled by the diffusion of oxygen atoms.

Acknowledgments

The authors are indebted Dr. K. Abe of Kobe Steel, Ltd., Hyogo, Japan for sample preparation and chemical analysis of the samples.

References

[1] S. Yamaguchi, J. Phys. Soc. Jpn., 24 (1968) 855.
[2] S. Hashimoto, J. Appl. Crystallogr., 8 (1975) 243.
[3] S. Yamaguchi and M. Hirabayashi, J. Appl. Crystallogr., 3 (1970) 319.

[4] S. Hashimoto, H. Iwasaki, S. Ogawa, S. Yamaguchi and M. Hirabayashi, J. Appl. Crystallogr., 7 (1974)67.
[5] M. Hirabayashi, S. Yamaguchi, T. Arai, H. Asano and S. Hashimoto, Phys. Status Solidi. A, 23 (1974) 331.
[6] T. Arai and M. Hirabayashi, J. Less-Common Met., 44 (1976) 291.
[7] T. Tsuji, M. Amaya and K. Naito, J. Therm. Anal., 38 (1992) 1817.
[8] T. Tsuji, M. Amaya and K. Naito, J. Nucl. Mater., 201 (1993) 126.
[9] T. Tsuji and M. Amaya, Thermochim. Acta, submitted.
[10] K. Naito, H. Inaba, M. Ishida, Y. Saito and H. Arima, J. Phys. E, 7 (1974) 464.
[11] T.B. Douglas, J. Nal. Bur. Stand., Sect. A, 67 (1963) 403.
[12] K. Naito, H. Inaba and S. Tsujimura, unpublished work.
[13] T. Matsui, T. Tsuji, T. Asano and K. Naito, Thermochim. Acta, 183 (1991) 1.
[14] T. Tsuji, M. Sato and K. Naito, Thermochim. Acta, 163 (1990) 279.
[15] S. Kaya and H. Sato, Proc. Phys. Math. Soc. Jpn., 25 (1943) 261.
[16] C. Sykes and F. W. Jones, Proc. R. Soc. London Set. A, 157 (1936) 213.
[17] S. Nagasaki, M. Hirabayashi and H. Nagasu, Nippon Kinzoku Gakkaishi, 13 (1949) 1.
[18] H. Sato and R. Kikuchi, Acta Metall., 24 (1976) 797.
[19] K. Gschwend, H. Sato and R. Kikuchi, J. Chem. Phys., 69 (1978) 5006.
[20] K. Gschwend, H. Sato, H. Iwasaki and H. Maniwa, J. Chem. Phys., 71 (1979) 2844.